

*Electronic Supplementary Information*

**Real-time observation of the photoionization induced water rearrangement dynamics in the 5-hydroxyindole–water cluster by time-resolved IR spectroscopy**

by

Mitsuhiko Miyazaki, Ayumi Naito, Takamasa Ikeda, Johanna Klyne, Kenji Sakota, Hiroshi Sekiya, Otto Dopfer, and Masaaki Fujii

*Contents*

**Figure S1.** Excitation schemes of IR spectroscopy employed in this study.

**Figure S2.** Time-of-flight mass spectrum of a5HI–W(NH).

**Figure S3.** One-color REMPI spectra of 5HI<sup>+</sup>–W obtained by picosecond laser pulses.

**Figure S4.** Expanded scan around the  $\nu_{\text{NH}}^{\text{free}}$  region of 5HI<sup>+</sup>–W clusters.

**Figure S5.** Potential energy curves for the torsional motion of the OH group of 5HI and 5HI–W.

**Figure S6.** Picosecond time-resolved IR spectra of a5HI<sup>+</sup>–W(NH) and a5HI<sup>+</sup>–W(OH) clusters.

**Figure S7.** TRIR spectra of a5HI<sup>(+)</sup>–W(NH) in the mid-IR region.

**Figure S8.** Theoretical IR spectra of a5HI and a5HI<sup>(+)</sup>–W water clusters in the mid-IR region.

**Figure S9.** Internal energy dependence of  $\nu_{\text{NOS}}$  and  $\nu_{\text{DOS}}$  of the a5HI<sup>+</sup>–W clusters.

**Figure S10.** Preliminary potential surface between the 5HI<sup>+</sup> cation and a water molecule.

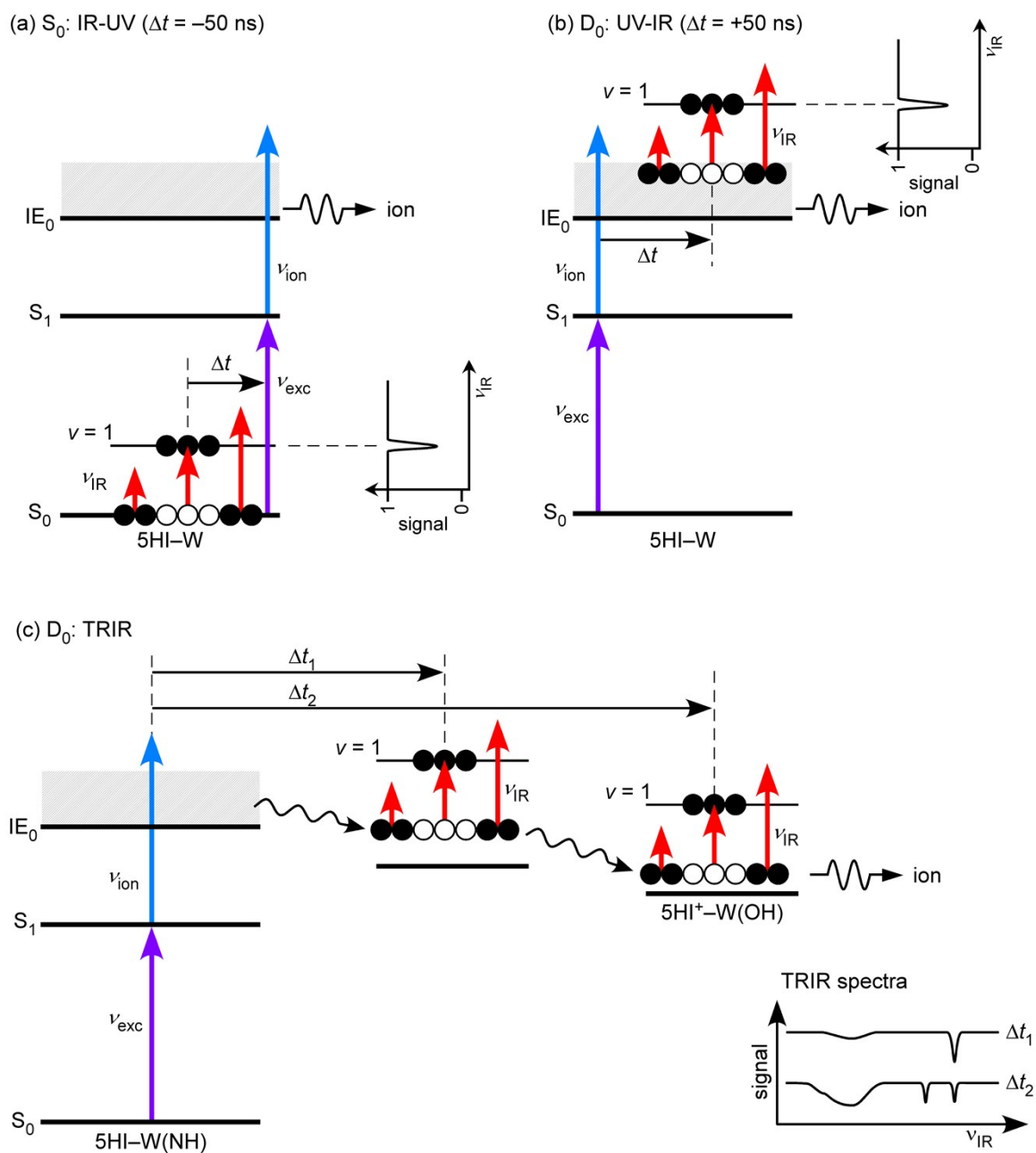


**Fig. S1** Excitation schemes used in the present work. a) IR-UV, b) UV-IR spectroscopies for static IR spectra in the  $S_0$  and  $D_0$  states, respectively. c) Time resolved IR spectroscopy in the  $D_0$  state.

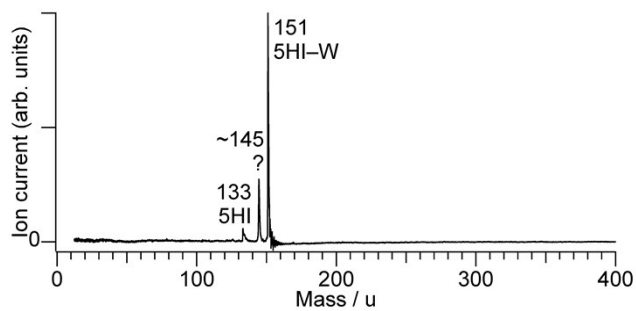


**Fig. S2** Time-of-flight mass spectrum measured by resonant two-color ionization *via*  $S_10^0$  band of a5HI-W(NH).  $\nu_{\text{ion}}$  was set to  $28184 \text{ cm}^{-1}$ . Unassigned mass at  $\sim 145 \text{ u}$  may be due to thermal- and/or photo-dissociation product, whose intensity depends on conditions.

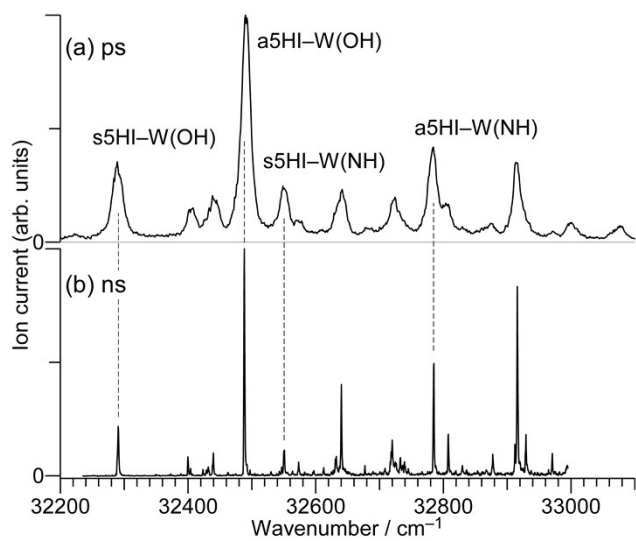


**Fig. S3** One-color REMPI spectra obtained in the  $5\text{HI}^+-\text{W}$  channel using Q-MS by (a) picosecond and (b) nanosecond laser pulses.

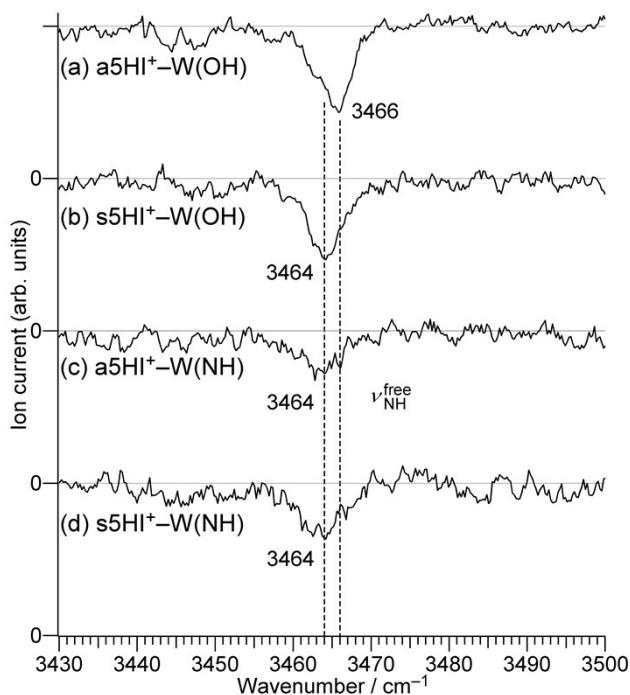


**Fig. S4** Expanded scan around the  $\nu_{\text{NH}}^{\text{free}}$  region of  $5\text{HI}^+-\text{W}$  clusters. For the NH-bound isomers, (c) and (d),  $\nu_{\text{NH}}^{\text{free}}$  appears as a signature of the isomerization product, the OH-bound isomer. For the OH-bound isomers, on the other hand, they are adiabatically ionized and hold the same structural motif as in the  $S_0/S_1$  states. One can notice from Fig. S3 that only  $a5\text{HI}^+-\text{W}(\text{OH})$  has a slightly higher frequency than others. This reproducible difference is only  $2\text{ cm}^{-1}$  because of little influence from the distant OH group on the NH bond. If the orientation of the OH group is conserved in the rearrangement reaction, the reaction product from  $a5\text{HI}^+-\text{W}(\text{NH})$  is  $a5\text{HI}^+-\text{W}(\text{OH})$ , and from  $s5\text{HI}^+-\text{W}(\text{NH})$  it is  $s5\text{HI}^+-\text{W}(\text{OH})$ . This means that  $\nu_{\text{NH}}^{\text{free}}$  within the same OH orientation,  $a5\text{HI}^+-\text{W}(\text{NH}/\text{OH})$  and  $s5\text{HI}^+-\text{W}(\text{NH}/\text{OH})$ , should match each other. In fact, for the  $s5\text{HI}^+-\text{W}(\text{NH}/\text{OH})$ , this prediction holds. However, for  $a5\text{HI}^+-\text{W}(\text{NH}/\text{OH})$ , the frequency differs, and  $\nu_{\text{NH}}^{\text{free}}$  of  $a5\text{HI}^+-\text{W}(\text{NH})$  matches with that of  $s5\text{HI}^+-\text{W}(\text{OH})$ . This observation suggests that the reaction product from  $a5\text{HI}^+-\text{W}(\text{NH})$  is  $s5\text{HI}^+-\text{W}(\text{OH})$ , *i.e.* an *anti*→*syn* rotation of the OH group also occurs in the course of the NH→OH water rearrangement. This *anti*→*syn* OH internal rotation is energetically possible, because  $s5\text{HI}^+-\text{W}(\text{OH})$  is more stable by  $\sim 100\text{ cm}^{-1}$  than  $a5\text{HI}^+-\text{W}(\text{OH})$ , but the barrier height for the rotation needs also to be considered. A relaxed potential curve of the OH torsional rotation is given in Fig. S4.

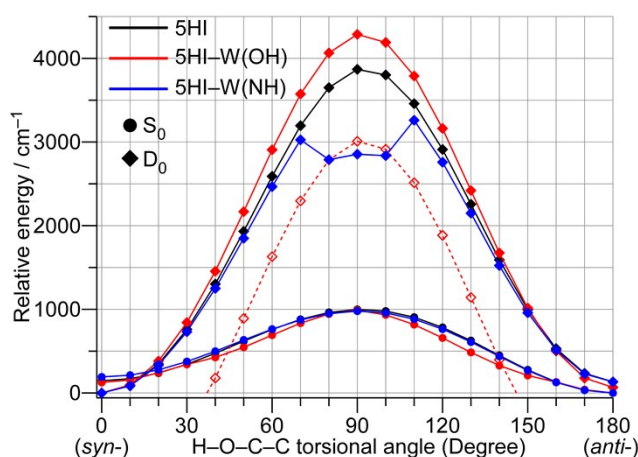


**Fig. S5** Potential energy curves for the torsional motion of the OH group of 5HI and 5HI-W in the neutral (circles) and cationic (squares) ground states. Red dashed line shows a shifted curve of the red solid line by  $-1277\text{ cm}^{-1}$ , which is the energy difference between the  $a5\text{HI}^+-\text{W}(\text{NH})$  and  $a5\text{HI}^+-\text{W}(\text{OH})$  isomers. The relaxed potential curves of the OH torsional motion were obtained by optimizing coordinates other than the H-O-C-C dihedral angle. The curves are not corrected for zero-point energies.

The torsional barriers in the  $S_0$  states are  $\sim 1000\text{ cm}^{-1}$  and those in the  $D_0$  state are  $3000\text{--}4000\text{ cm}^{-1}$  with almost no hydration effects. The increases of the barrier height upon ionization of 5HI reflect a higher double bond character of the C-O bond in the  $D_0$  state. A strange behavior in  $5\text{HI}^+-\text{W}(\text{NH})$  would be the interaction with higher electronic states. Because  $a5\text{HI}^+-\text{W}(\text{OH})$  is more stable by  $1277\text{ cm}^{-1}$  than  $a5\text{HI}^+-\text{W}(\text{NH})$ , the OH torsional barrier of the OH-bound isomer can be lowered by  $1277\text{ cm}^{-1}$  and thus the energy barrier from  $a5\text{HI}^+-\text{W}(\text{NH})$  becomes  $2000\text{--}3000\text{ cm}^{-1}$ . This energy is lower than the maximum internal energy that can be implemented by total energy of the photoionization according to the PIE curve.<sup>1</sup> This may allow the OH rotation during the water rearrangement. However, even that is the case, most of the cluster ions are expected to be populated lower than the torsional barrier, resulting in a coexistence both  $a5\text{HI}^+-\text{W}(\text{OH})$  and  $s5\text{HI}^+-\text{W}(\text{OH})$  as the rearrangement products. A conformational change of related molecule has recently been reported by Lopes Jesus *et al.* for photoexcitation of matrix-isolated 5-methoxyindole (5MI), in which the hydrogen atom of the OH group of 5HI is substituted to a methyl group.<sup>2</sup> They concluded that the rotation of the methoxy group occurs in the  $S_0$  state after internal conversion from the  $S_1$  state, because the barrier height for the torsional isomerization in the  $S_1$  state ( $\sim 1800\text{ cm}^{-1}$ ) is rather high comparing to that in the  $S_0$  state ( $\sim 500\text{ cm}^{-1}$ ). To accurately address the final distribution of the product isomers, much more precise estimation of the torsional barrier height and internal energy distribution after ionization in combination with MD simulation is necessary. A similar rotation of the OH group would also be possible in the  $\text{NH}\leftarrow\text{OH}$  water rearrangement of the initially OH-bound isomers. However, no significant difference is seen in  $\nu_{\text{OH}}^{\text{free}}$  because of very weak intensities of  $\nu_{\text{OH}}^{\text{free}}$  resulting from the low reaction yield in this direction and the somewhat broader feature of  $\nu_{\text{OH}}^{\text{free}}$  than  $\nu_{\text{NH}}^{\text{free}}$ .

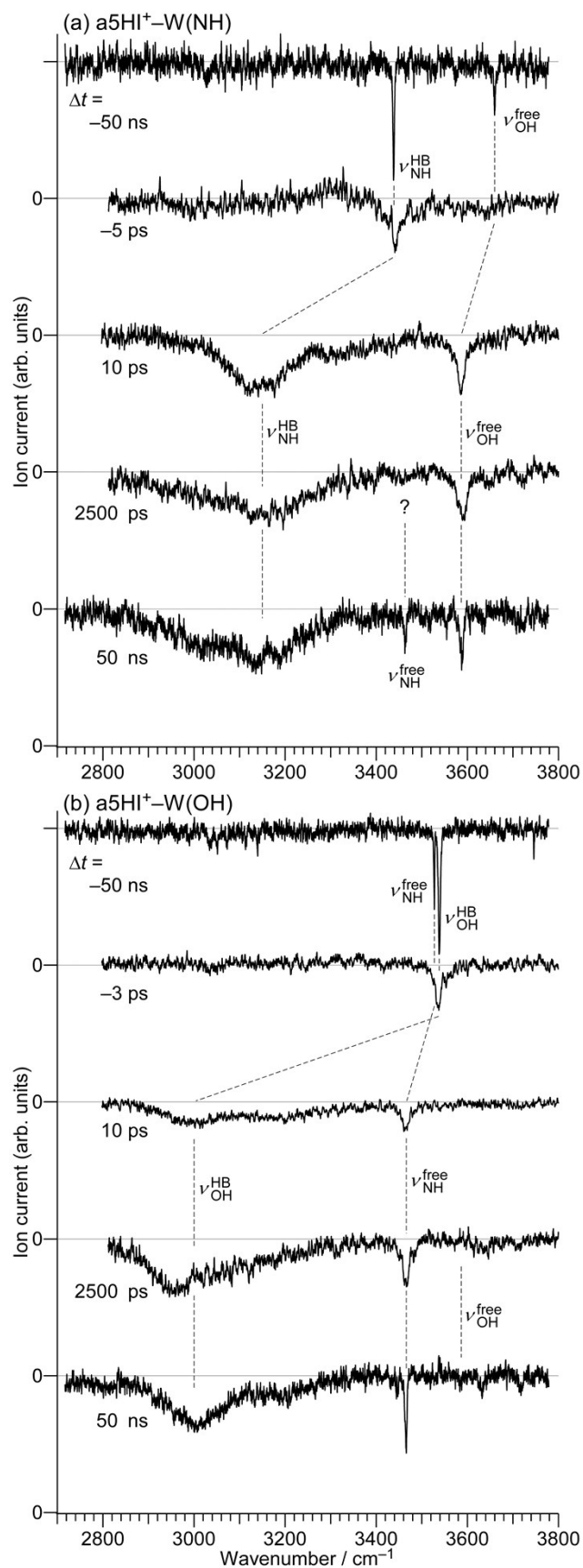


**Fig. S6** Picosecond TRIR spectra of (a)  $a5\text{HI}^+-\text{W}(\text{NH})$  and (b)  $a5\text{HI}^+-\text{W}(\text{OH})$  clusters obtained monitoring one-color ionization signal. IR spectra at  $\Delta t = \pm 50$  ns are stationary IR spectra reproduced from Fig. 4 for comparison.

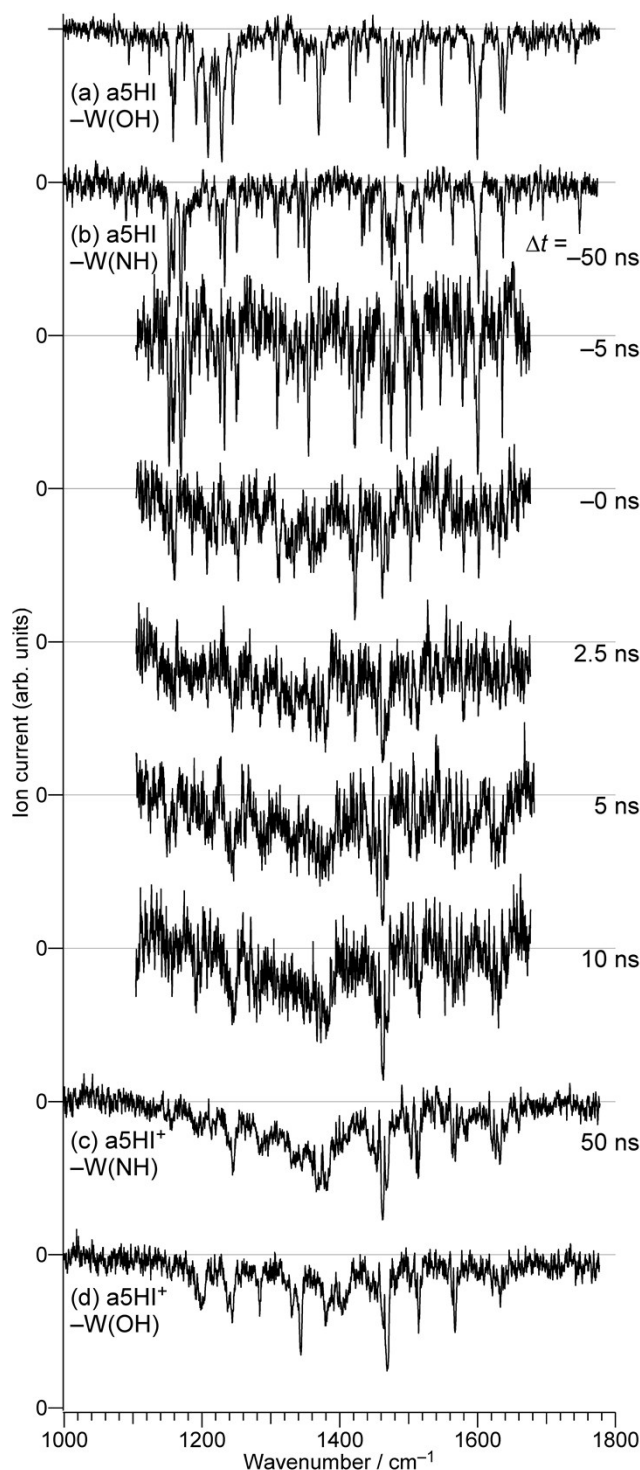


**Fig. S7** Stationary IR spectra of (a) a5HI–W(OH) and (d) a5HI<sup>+</sup>–W(OH) clusters, and (b) TRIR and (c) stationary IR spectra of a5HI<sup>+</sup>–W(NH) in the mid-IR range.  $\nu_{\text{ion}}$  was set to 36353 cm<sup>-1</sup>. In this range, the C–O–H bending vibration ( $\beta_{\text{COH}}$ ) was expected to be a characteristic vibration of the reaction product, because  $\beta_{\text{COH}}$  is known to show a blue-shift by forming a hydrogen bond. The IR spectra show a number of bands, but transitions around 1200 cm<sup>-1</sup> for the S<sub>0</sub> state and around 1400 cm<sup>-1</sup> for the D<sub>0</sub> state can be thought to carry mainly the  $\beta_{\text{COH}}$  character according to theoretical IR spectra shown in Fig. S7 (see below). There are some differences between the mid-IR spectra of a5HI<sup>+</sup>–W(NH/OH), however, overlap of bands due to similarity of spectra and broader background contributions probably due to the internal energy make it difficult to find a specific transition for the OH-bound product isomer.

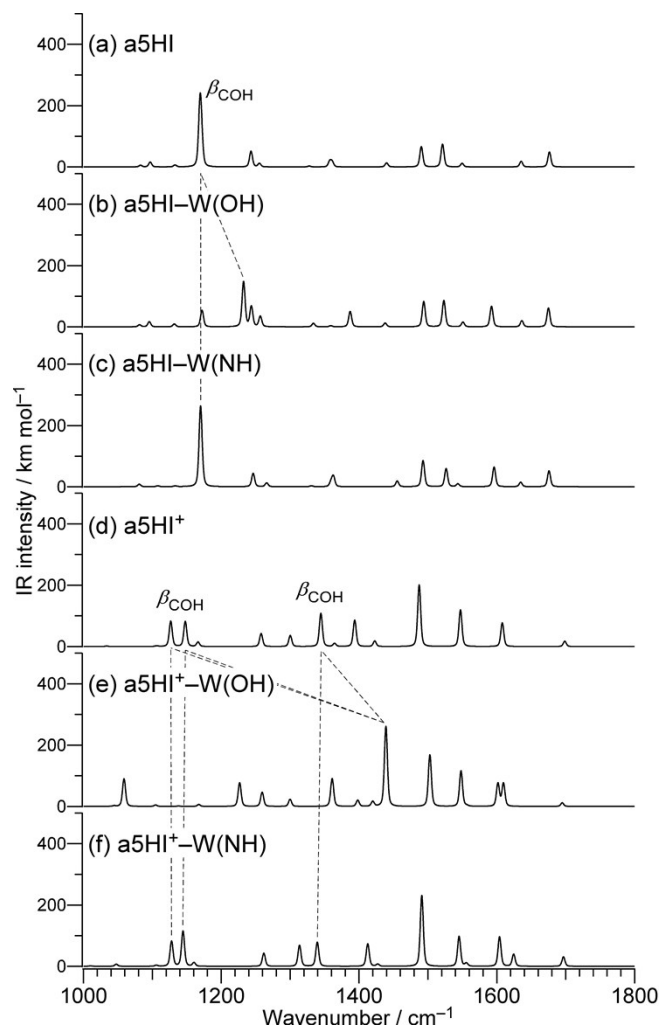


**Fig. S8** Theoretical IR spectra of a5HI and a5HI-W clusters in the  $S_0$  and  $D_0$  states in the mid-IR range calculated at the CAM-B3LYP/cc-pVTZ level with GD3BJ empirical dispersion correction. The harmonic frequencies are scaled by 0.98 and convoluted by a Voigt profile with  $\sim 5$   $\text{cm}^{-1}$  width. Vibrations that strongly wear the C-O-H bending character ( $\beta_{\text{COH}}$ ) are indicated by dashed lines. In the  $D_0$  state, the  $\beta_{\text{COH}}$  character is delocalized due to couplings with other vibrations.

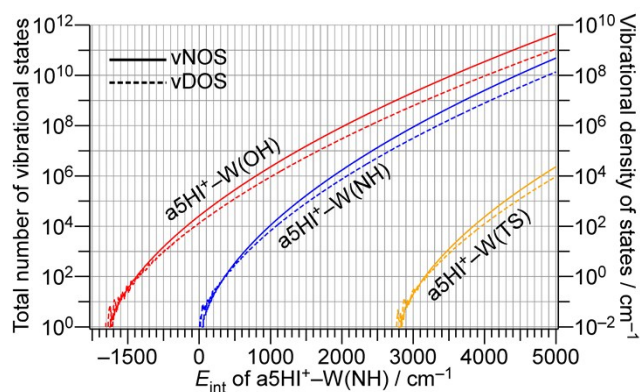


**Fig. S9** Internal energy dependence of the total number of vibrational states (vNOS, solid lines) and vibrational density of states (vDOS, dashed lines) of initial (blue), final (red), and transition (yellow) states. Relative energies of the transition state  $E^\ddagger = 2744 \text{ cm}^{-1}$  and the OH-bound isomer  $E_{\text{OH}} = -1322 \text{ cm}^{-1}$  from the NH-bound isomer, and unscaled harmonic frequencies were used to evaluate the curves.

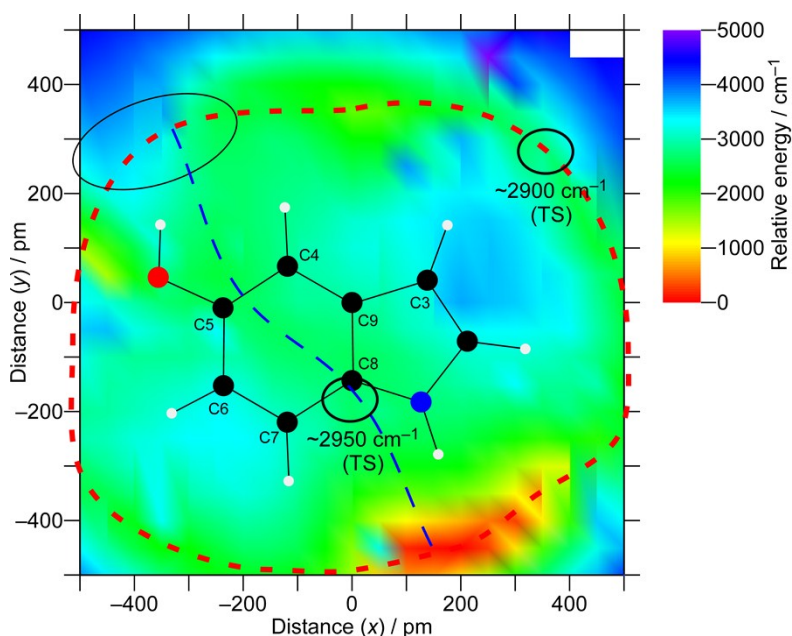


**Fig. S10** Preliminary potential energy surface (PES) between the  $5\text{HI}^+$  cation and a water molecule calculated at the CAM-B3LYP/cc-pVTZ level with GD3BJ empirical dispersion correction. ZPE and BSSE corrections have not been taken into account. The OH-bound structure does not give a minimum erroneously due to an OH torsional isomerization during the calculations (see below). In addition to the in-plane circulating path (red dashed line) that is described in the main text, an out-of-plane path (blue dashed line) can also be seen. This path appears between the negatively charged carbon atoms C4, and C6, C7, because they repel the negative oxygen atom of the water molecule, while C8, C9, and C5 are positively charged. Both paths show similar barriers ( $<3000 \text{ cm}^{-1}$ ) for the NH $\rightarrow$ OH rearrangement reaction. The barrier height for the in-plane path is slightly different from that obtained by calculations performed in the main text due to the lack of ZPE corrections. In the course of the calculations, the carbon atom C9 was fixed at the origin of the coordinate system ( $x = 0, y = 0, z = 0$ ), C8 was restricted within the vertical axis ( $x = 0, z = 0$ ), and C3 was confined in the plane ( $z = 0$ ). The molecular plane of  $5\text{HI}^+$  then can be kept almost in the x-y plane, except for the hydrogen of the OH group, which points toward the water molecule when it come close to the

OH group. Then, the oxygen atom of the water molecule ( $O_W$ ) was put on a position  $(x_i, y_i)$ . Hydrogen atoms of the water molecule are always positioned on the opposite side to the  $5HI^+$  cation to maximize the charge-dipole interaction. From this initial geometry, all other degrees of freedom were optimized ( $y$  of C8,  $x$  and  $y$  of C3,  $z$  of  $O_W$ , orientation of the water molecule, torsional angle of the OH group, and so on). Then,  $O_W$  is moved to a next position  $(x_{i+1}, y_{i+1})$ . A step size of 50 pm was adopted, and  $20 \times 20 = 400$  positions were mapped in total. The OH-bound well (a region around  $x = -400$  pm,  $y = 300$  pm; shown by a circle) did not give an energy minimum because an *anti*→*syn* OH-rotation occurred during the automatic scan of the  $O_W$  positions in the Gaussian program. At almost all calculated positions, optimization criteria (opt = tight) were not achieved, though energy changes at end of every optimization step were very small reflecting a rather flat PES on the  $\pi$  ring.

### References

1. T. Ikeda, K. Sakota and H. Sekiya, *J. Phys. Chem. A*, 2016, **120**, 1825-1832.
2. A. J. Lopes Jesus, R. Fausto and I. Reva, *J. Phys. Chem. A*, 2017, **121**, 3372-3382.